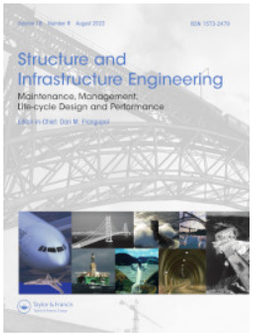

Taylor & Francis
Taylor & Francis Group

Structure and Infrastructure Engineering
Maintenance, Management, Life-Cycle Design and Performance

ISSN: (Print) (Online) Journal homepage: https://www.tandfonline.com/loi/nsie20

Measurements of bridge dynamic amplification factor using bridge weigh-in-motion data

Jan Kalin, Aleš Žnidarič, Andrej Anžlin & Maja Kreslin

To cite this article: Jan Kalin, Aleš Žnidarič, Andrej Anžlin & Maja Kreslin (2022) Measurements of bridge dynamic amplification factor using bridge weigh-in-motion data, Structure and Infrastructure Engineering, 18:8, 1164-1176, DOI: 10.1080/15732479.2021.1887291

To link to this article: https://doi.org/10.1080/15732479.2021.1887291

Published online: 26 Feb 2021.

STRUCTURE AND INFRASTRUCTURE ENGINEERING
2022, VOL. 18, NO. 8, 1164–1176
https://doi.org/10.1080/15732479.2021.1887291

Measurements of bridge dynamic amplification factor using bridge weigh-in-motion data

Jan Kalin, Aleš Žnidarič, Andrej Anžlin and Maja Kreslin

Slovenian National Building and Civil Engineering Institute, Ljubljana, Slovenia

ABSTRACT

The dynamic component of bridge traffic loading is commonly taken into account with a Dynamic Amplification Factor (DAF)—the ratio between the dynamic and static load effects on a bridge. In the design codes, this factor is generally more conservative than in reality. Recently a new method of calculation of this factor had been developed. Data from 15 different bridges have been analysed since then and this paper presents the results of the analyses. The background for Bridge Weigh-in-Motion is given, and the most recent method for DAF calculation is described. The sites from which the data originated are presented, and the selection of data discussed. The results of the analyses are presented and discussed and some examples of DAF calculations are shown. Data from the considered sites have invariably demonstrated a DAF decrease with increasing axle load. This is a significant result, especially for assessment of existing structures, since it is beneficial to use measured structural parameters to optimise structural analysis.

ARTICLE HISTORY
Received 29 May 2020
Revised 14 October 2020
Accepted 17 December 2020

KEYWORDS
Bridge loads; Bridge maintenance; Bridge Weigh-in-Motion; Building codes; Dynamic Amplification Factor; Dynamic analysis; Measurement; Traffic loading;

1. Introduction

Proper assessment of the behaviour of bridges under traffic load is of vital importance for the improvement of the design techniques for new structures and for evaluations of the condition of existing ones. At the same time, it is accepted that shortfalls exist in the determination of the traffic loads which a bridge must support during its expected lifetime. A common reason is, amongst other factors, insufficient understanding of the complex dynamic interaction between the bridge and the heavy crossing vehicles. This interaction is usually simplified into a parameter called the Dynamic Amplification Factor (DAF), or sometimes the Dynamic Increase Factor (DIF). In general, the degree of dynamic loading is defined with a coefficient that describes the relationship between the total response observed on a structure during dynamic loading and its corresponding static component.

The design codes prescribe relatively high and conservative dynamic allowance factors. This is even more pronounced if, according to the design codes, the extreme static load effects are multiplied with a high value of DAF. The positive side of the conservative design is that, after many years in service and despite deterioration and increasing traffic loading, the bridges likely still have sufficient capacity to carry the current traffic. These extra reserves in structural safety are greatly appreciated, especially when the bridges are damaged and when replacement or lengthy repair would result in a substantial burden for the users.

Therefore, the reliability analysis of an existing bridge should be based on accurate information. This includes hidden reserves in bridge behaviour, for example, how it performs under loading. For bridges, one of the critical loadings comes from traffic. If the aim is optimal assessment, it is essential to replace the conservative load models from the codes with the ones that are calculated from actual heavy freight vehicle loading data, static and dynamic. Having such information can draw a dividing line for further actions, which can spread from doing nothing to various levels of rehabilitation measures and even replacement of a bridge.

Dynamic impacts due to traffic load are most often calculated at mid-span where the maximum sagging moments occur. However, a variety of alternative definitions also emerged because the maximum static and maximum dynamic responses of the bridge do not necessarily happen at the same loading position. Many authors have evaluated the dynamic components of traffic load analytically. In their numerical simulations of multi-span continuous bridges, González and Mohammed (2018) observed notable differences between DAF of the mid-span sagging moment and the hogging moment over the internal support. Additionally, oscillations may occur in sections far from the mid-span, with a significant difference in magnitude. In such cases, Cantero, González, and O'Brien (2009) proposed the so-called Fully Dynamic Amplification Factor (FDAF), which is equal to the maximum total load effect across the bridge

CONTACT Jan Kalin jan.kalin@zag.si Slovenian National Building and Civil Engineering Institute, ZAG Ljubljana, Dimičeva 12, 1000 Ljubljana, Slovenia

length, divided by the highest static load effect at a particular reference section, typically chosen at the mid-span.

In one of the early studies, Wright and Green (1964) concluded that the DAFs computed from measured deflections were always higher than the corresponding factors computed from the measured strains. On the other hand, in their numerical study of the dynamic response of a slab bridge, Humar and Kashif (1995) showed that DAF values calculated from deflections or strain measurements matched, if they took into account only the first mode shape of a bridge. When they included higher mode shapes, they could not predict whether the DAF values would increase or decrease. They only established that the two values were close to each other.

The article begins with an overview of the use of DAF in codes and guidelines and a description of some methods for measuring DAF. Subsequent sections briefly describe the B-WIM method for measuring traffic loading and the evolution of DAF calculation method. The proposed method and DAF results from fifteen test sites are presented and discussed. The article concludes with recommendations for selecting the DAF factor.

2. A brief history of DAF in guidelines

The three factors most often associated with an oscillating bridge are its span, natural frequencies and road surface irregularities. However, several other parameters affect the dynamic response of a bridge (Alois, Croce, Sanpaolesi, & Gerhard, 1996). They depend on the traffic characteristics, primarily the velocity, axle loads, configuration and dynamic characteristics of the vehicles, and on the characteristics of the bridge, its type, soil-structure interaction, condition of the main structural members, expansion joints and bridge supports, and its damping response to the loading.

The importance of dynamic bridge loading was already recognised in the 1930s, when the British provision Standard Loading Code incorporated the dynamic factor of 1.5 (González & Žnidarič, 2009). In the same period, the American Association of State Highway and Transportation Officials (AASHTO, 1928) issued Standard Specifications for Highway Bridges and introduced the first relation between the length of the bridge and DAF. Its value was limited to 1.25 and was changed to 1.3 in 1989 (AASHTO, 1989). Other design codes in the 1930s, like the one issued by the Kingdom of Yugoslavia (1936), adopted similar formulas, according to which DAF values decreased with the increasing bridge span.

Other guidelines and codes of practice, such as the Ontario Bridge Design Code (Ministry of Transportation & Communication, 1983), correlated the dynamic allowances with the first natural frequency of the bridge. In their subsequent editions, they mostly abandoned the frequency-based approach, firstly, to simplify the design procedures, and secondly, due to appreciation that a large number of other factors affect the dynamic bridge response. McLean and Marsh (1998) defined three different DAF classes related to the bridge surface roughness: for bridges with smooth approach

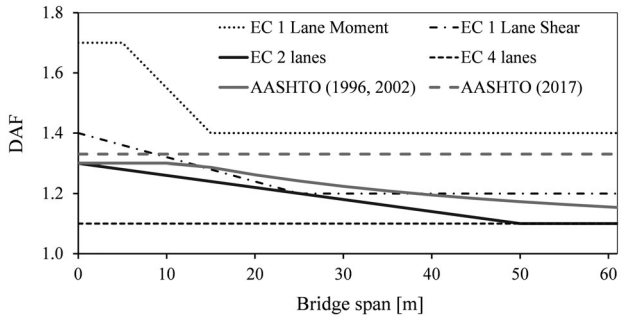

Figure 1. DAF allowances from the AASHTO (1996, 2017) and Eurocode 1-2 (CEN, 2003) codes.

(DAF = 1.1), with rough surface with bumps (DAF = 1.2) and with poor road surface (DAF = 1.3). In all cases for bridges with spans shorter than 12 m.

The Swiss code now requires smooth road surfacing approaches on a bridge as a standard, since poor quality road surfaces can result in substantial increases in the dynamic component of load effect (González & Žnidarič, 2009). The same issue was addressed in the Eurocode (CEN, 2003). The dynamic load amplification is indirectly integrated in the Load Model 1, but for the pavement of good quality. In case of fatigue life assessment for road bridges based on the recorded traffic, the axle loads should be multiplied by a factor of 1.2 or 1.4, for the surfaces of good and medium roughness, respectively (CEN, 2003). Furthermore, the code conservatively recommends an additional amplification factor of 1.3 for any cross-section within 6 m from the expansion joint, when fatigue issues are considered, and also allows the modification of this value in the National Annex.

Figure 1 displays the four DAF vs bridge span functions which were integrated into the Eurocode's load model 1, and relate to different load effects and traffic regimes. Additionally, the latest recommendation from the bridge design specification AASHTO (1996) is shown. Later in the paper, the results of DAF measurements are compared to these criteria.

Due to the complex dynamic response of bridges, which can be challenging to model (Caprani, 2005), the authors of this paper propose evaluating the DAF, wherever possible, from the results of B-WIM measurements, which collect the dynamic responses of the bridge induced by the entire traffic flow.

3. Measuring DAF

In the early days, the static and dynamic responses of bridges were measured to calibrate the bridge codes and to compare the measured bridge performance with the predictions of the design. Cantieni (1984), for example, reported about the dynamic load tests on highway bridges in Switzerland that went back to the mid-1920s. Measurements were parts of load tests and were mostly performed on new bridges still closed to traffic. A limited number of pre-weighed vehicles, typically empty and fully loaded, crossed the bridge at two to three different speeds, with or without an obstacle just before the bridge, which amplified the

dynamic response of the structure. Such load tests were, and still are, common in many countries (Casas, Olaszek, Šajna, Žnidarič, & Lavrič, 2009).

The issue with this approach is that the limited selection of vehicles used in the test cannot give a complete picture of the bridge performance under changing traffic, structural and environmental conditions. Furthermore, in such dynamic tests, the test vehicles are significantly lighter than the extreme cases found in traffic, which leads to excessively high DAF values. These DAF values, when combined with modelled extreme static loads, yield conservative maximum load effects. These are appreciated in the design of new bridges, as they guarantee additional robustness when they age and deteriorate. However, they are less suitable for the analysis of existing bridges because they may unnecessarily lead to results that require more severe and more costly measures than are necessary.

More reliable DAF measurements became available only after the development of Bridge Weigh-in-Motion (B-WIM) systems. These systems can correlate the structural responses with the loading of all crossing vehicles and therefore take into consideration a much larger variety of dynamic loading cases. One of the earliest attempts to evaluate dynamic bridge performance with B-WIM was made by Ghosn and Xu (1989). They were looking for the dominant vibration frequencies on the end girders, using a Fourier analysis of the strain record. They assumed that the end girders carry little static, but considerable dynamic effect. The measured frequencies determined the dynamic 'influence lines', with amplitudes calculated using the minimisation-of-error technique of the B-WIM algorithm. Preliminary results indicated that the proposed method could be applicable for a large number of bridges where more traditional methods fail to predict the dynamic effects. At the same time, Bakht and Pinjarkar (1989) used a modified definition of dynamic amplification, in which they approximated the static deflection of the bridge from the so-called median response of the bridge obtained from the dynamic response of the structure.

A few years later, Nassif and Nowak (1995; 1996) made the first more extensive measurements of dynamic behaviour under random traffic. They coupled a dedicated acceleration measurement system with a commercially available B-WIM system and evaluated the dynamic amplification by comparing the dynamic signal with the static B-WIM approximation on four bridges with spans from 9 to 24 m. They approximated the static part of the signal, ε_{stat}, by filtering the measured or total signal, ε_{tot}, with a Fourier Transformation. The filtering parameters were selected based on the experience of the researchers. The dynamic effect was described with a Dynamic Load Factor, DLF, also denoted as DLA (dynamic load allowance), of the form:

$$DLF = \frac{\varepsilon_{tot} - \varepsilon_{stat}}{\varepsilon_{stat}} = \frac{\varepsilon_{dyn}}{\varepsilon_{stat}}. \quad (1)$$

A few tens of DLFs were calculated on each bridge, for each girder, and were presented as a function of maximum static stress. The authors concluded that the dynamic component of stress or strain (the dynamic increment, ε_{dyn}) is practically independent of the static component and that, as a result, the DLF decreased with increasing static stress/strain. Furthermore, they noted that for very heavy trucks, DLF did not exceed the theoretical results. Two years later, Kirkegaard, Neilsen, and Enevoldsen (1997) came to similar conclusions by calculating the dynamic impact factors from selected simulated truck crossing scenarios. These results were the primary data source for the DAF recommendations in the Danish Reliability-Based Bridge Assessment (RBBA) code (DRD, 2004).

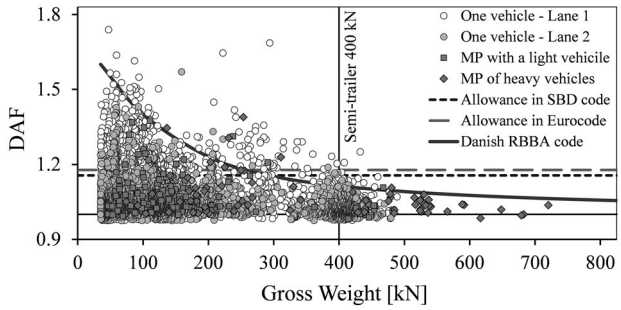

Figure 2. Results of early DAF measurements, from (Žnidarič et al., 2006).

Work on using B-WIM to evaluate dynamic loading did not continue until the SAMARIS project (Žnidarič et al., 2006). The maximum static response, ε_{stat}, was calculated by multiplying the B-WIM generated axle loads and the influence lines (Žnidarič, Lavrič, & Kalin, 2008). The DAF was defined as:

$$DAF = \frac{\varepsilon_{tot}}{\varepsilon_{stat}}, \quad (2)$$

where ε_{tot} represents the maximum total, i.e. dynamic and static response of the structure. However, errors of the calculated axle loads yielded excessive and unrealistic DAF values. Consequently, the data evaluation required thorough visual quality checks that eliminated all unreliable results. The first DAF calculation test was performed on a 30 m long simply-supported span, a part of multi-span beam-and-slab bridge. Each dot in Figure 2 represents one of the 5260 results divided according to the vehicles that triggered each event. Included were single trucks in each of the two lanes and multiple presences (MP) of one heavy and one light and of two heavy vehicles. Heavy vehicles were taken as those weighing over 3.5 tonnes.

The results were promising, complied nicely with the numerical prediction of DAF from the Danish Road Directorate document (DRD, 2004) and demonstrated considerably lower DAF values than the allowances in the Slovene bridge design (SBD) code used at the time of construction, and Eurocode. However, the evaluation procedure involved too much manual work to be of practical value. Thus, the ARCHES project (González & Žnidarič, 2009) reinvestigated the possibilities of conditioning the strain signals with various filters to approximate the static response of the bridge. Equation (2) changed slightly to:

$$DAF = \frac{\varepsilon_{tot}}{\varepsilon_{qstat}}, \quad (3)$$

to reflect the fact that the generally unobtainable static response was replaced with a quasistatic response.

The report compared the current building code recommendations for dynamic allowances with the simulation and B-WIM measurement results on several bridges. It reconfirmed that the design recommendations for dynamic allowance values were mostly conservative, especially at extreme traffic loads. For the analysis of existing bridges, the authors recommended the use of more accurate methods based on measurements. In the following years, the DAF calculation procedure based on B-WIM measurements has been developed further (Kalin, Žnidarič, & Kreslin, 2015). This article presents its latest improvements and demonstrates its efficiency and robustness based on the analysis of data from 15 different bridges.

Before proceeding to the description of the DAF measurement from Bridge Weigh-in-Motion data, it should be noted that there are several definitions of DAF. A good review of DAF definitions is given in Bakht and Pinjarkar (1989). Eight definitions from literature dealing with DAF are summarized and each of them used to obtain DAF from the same set of data. It was shown that the results can differ strongly among themselves. The authors noted that none of the definitions was rigorously justified in the respective papers and proposed a method of obtaining the approximation to static values, which is very close to the one used in this paper and described in Equation (3). In view of the large amount of data at our disposal, we plan to investigate the consequences of different DAF definitions in further research.

4. Bridge weigh-in-motion for measurement of the dynamic amplification factor

Bridge Weigh-in-Motion (B-WIM) systems transform the existing bridges or culverts from the road network into weighing scales (Corbally et al., 2014; Moses, 1979). The B-WIM algorithm uses the strains measured on a bridge or culvert superstructure to calculate the axle loads of the crossing vehicles. On suitable structures with smooth pavement, high accuracies of the weighing results are achieved—up to less than 5% error for 95% of the axle loads (Jacob, O'Brien, & Jehaes, 2002; O'Brien & Žnidarič, 2001).

For a B-WIM installation, the structures are mostly instrumented with strain measuring devices. Traditionally, strains are acquired on the main longitudinal members of a bridge to provide response records of the structure under the moving vehicle load, but other locations can be used to improve the results. On slab bridges the strain sensors are typically mounted at the mid-span, across the entire width of the bridge at regular intervals. Measurements during the whole vehicle crossing over the structure provide redundant data, which facilitates the evaluation of axle loads. The top left corner of Figure 3 displays an enlarged photo of the strain transducer, with 200 mm base, that was used at all test sites, except for the two bridges instrumented for permanent monitoring, where strain gauges were glued directly to the concrete beams.

For most bridges the individual axles of the vehicles are detected with sensors mounted underneath the bridge

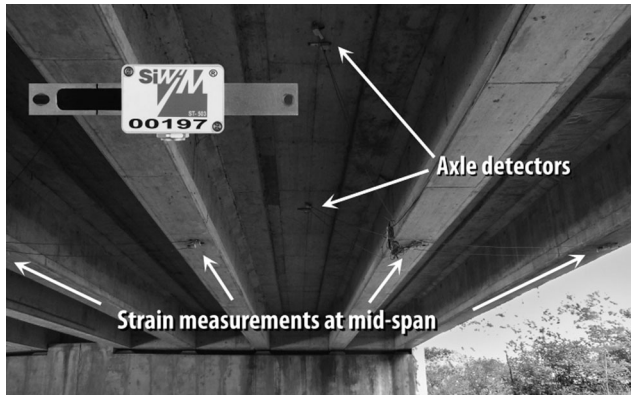

Figure 3. B-WIM instrumentation of a beam-and-slab bridge.

(Figure 3). They are installed in pairs, one for each traffic lane, 3 to 5 m apart in the direction of traffic. If they cannot provide signals with clearly distinguishable spikes at the locations of individual axles, to allow calculation of the axle spacings, they are replaced by the axle detectors on the upper side of the bridge (Žnidarič, Kalin, & Kreslin, 2018).

4.1. Theoretical background for B-WIM

The first step in the weighing procedure selects and combines parts of a continuous stream of measured data into the so-called events, which contain signals from one or more vehicles whose influences on the bridge overlap. Axles of vehicles within events are then identified, their velocities calculated, and the individual axles joined into vehicles. Finally, the N unknown axle weights A_i in each event are calculated from a system of M equations:

$$g(t_j) = \sum_{i=1}^{N} A_i I(v_i(t_j - t_i)); \; j = 1 \ldots M, \tag{4}$$

where $g(t_j)$ are the bridge responses measured at M different times and $I(x) = I(v_i(t_j - t_i))$ is the known influence line at location x. Axle velocities v_i and the arrival times of individual axles t_i determine the location of each axle at time t_j.

The inputs from all strain sensors are normally used, to minimise the influence of the varying transverse positions of vehicles. With a sampling rate of 512 samples per second and a typical vehicle crossing time of a few seconds, the number of equations is typically two orders of magnitude larger than the number of unknowns. This over-determined system of equations is solved for A_i, in the least-square sense, using the singular value decomposition algorithm (Press, Teukolsky, Vetterling, & Flannery, 2007).

Influence lines are defined as the response of the bridge, at the sensor location, to the passage of a unit axle load. They are the critical structural parameter that directly affects the quality of B-WIM measurements. For the last 20 years, B-WIM systems use influence lines derived directly from the measured data on the site (Žnidarič & Lavrič, 2010; Žnidarič, Lavrič, & Kalin, 2010). The influence line calculation method developed at the Slovenian National Building and Civil Engineering Institute (ZAG) uses equation (4),

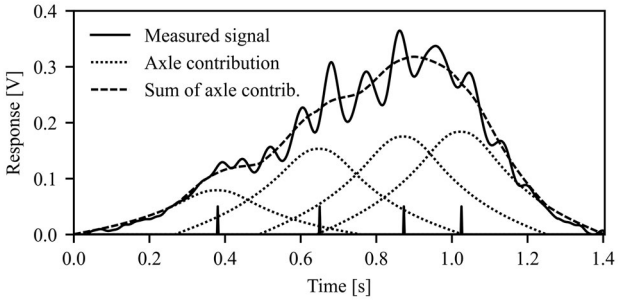

Figure 4. An example of B-WIM weighing results during the passage of 4-axle truck.

where the function $I(x)$ is also unknown and is calculated using Powell's minimisation technique (Press et al., 2007). The possibility of calculating actual influence lines is very helpful in analysing of existing bridges (Žnidarič & Kalin, 2020). Details of the influence line calculation procedure are given in Žnidarič et al. (2018).

Figure 4 presents an example of the weighing result of a 40.5 t 4-axle truck passing over a 10.5 m integral concrete slab bridge at 50 km/h. The solid trace is the sum of measured strain signals, the black spikes at the bottom are the positions of the four detected axles, the dotted traces are the influence lines at axle positions, multiplied by the axle loads, and the dashed trace is the sum of these axle contributions.

In the some of the response diagrams, such as the one on Figure 4, the values on the ordinate are given in volts, as supplied by the measurement system, since the exact conversion factor from the measured voltage to strains was, in some cases, not known. For the purpose of obtaining axle loads this is irrelevant, since the 'raw' values A_i are later multiplied by calibration factors. These factors are obtained from a few tens of passages of one or more calibration vehicles with known axle weights and determine the values with which the raw loads from Equation (4) are multiplied to obtain the real loads (Jacob et al., 2002). The measurement unit is also irrelevant for the calculation of DAF, which is a dimensionless ratio.

4.2. Measuring DAF with B-WIM

The B-WIM systems used for this work are based on the measurements of flexural strains of a bridge. In the SAMARIS project (Žnidarič et al., 2006), a procedure was developed that for the first time automatically calculated the DAF values, according to Equation (2). The maximum total strains, ε_{tot}, were measured for every vehicle crossing and the corresponding static load effects, ε_{stat}, were calculated by multiplying the influence line by the sum of the calculated axle loads, represented with the dashed trace in Figure 4.

The disadvantage of this method was that the miscalculated axle loads influenced the DAF values significantly. The two main sources of errors were misidentified axles and the ill-conditioning of the system of equations, which is a common issue on bridges with longer influence lines (Žnidarič et al., 2018). Unfortunately, the axle load errors are more frequent on bridges susceptible to dynamic excitation from traffic loading, which are precisely the cases, where the DAF values need to be calculated as accurately as possible.

Consequently, the DAF calculation methods examined in the ARCHES project assumed that the static and dynamic components of the load effect could be separated based on their characteristic frequencies. The characteristic frequency of the dynamic component needed to be higher than the frequencies present in the static component. The signal was transformed into the frequency domain using Fourier Transform (Press et al., 2007), the spectrum was low-pass filtered at a pre-determined cut-off frequency, and was retransformed into the time domain. Whatever remained was taken as the static load effect and used in the calculation of the DAF value.

The disadvantage of this method was that it was experience-based. An expert selected the parameters by looking at many bridge response signals and chose the cut-off frequency that best removed the dynamic portion of the signal without significantly affecting the static component of the bridge response. This method gave valuable results but was not suitable for broader application, because it required the use of unique, specialised expertise.

4.3. Two-pass calculation of DAF

To overcome the subjectivity issue, a modified DAF calculation method (Kalin et al., 2015) processes each of the K loading events twice, first to obtain the filtering parameters and the second time to calculate DAFs. The insight is that, while the ε_{stat} values calculated directly with the B-WIM algorithm can sometimes be wrong, on average they represent a good approximation of the static response of the bridge, which is the assumption in the original B-WIM article (Moses, 1979). As such, they can be used as a target for fitting the low-pass filter cut-off frequency. Once the mean cut-off frequency is known, the more robust method, based on the Fourier Transform, can be used to obtain the quasi-static response.

During the first pass, the N individual axle loads A_i are first determined using Equation (4) and then the optimal low-pass filter cut-off frequency $f_{o,k}$ for the kth event is determined by minimising:

$$\chi^2(f_{0,k}) = \sum_{j=1}^{M}\left[g'\left(t_j|f_{0,k}\right) - \sum_{i=1}^{N} A_i I(v_i(t_j - t_i))\right]^2 \qquad (5)$$

with respect to $f_{o,k}$, where $g_k{}'\left(t_j|f_{0,k}\right)$ is the filtered measured response and the values A_i are fixed to the previously determined values.

A typical B-WIM installation sums the values from strain sensors across the entire width of the structure, to obtain vehicle weights that are as independent of the transverse position of the vehicle as possible. For DAF measurements, however, only a few sensors with the highest responses are used. The reasoning behind this choice is that the inclusion of sensors away from vehicle locations decreases the signal-to-noise ratio without increasing the DAF-related

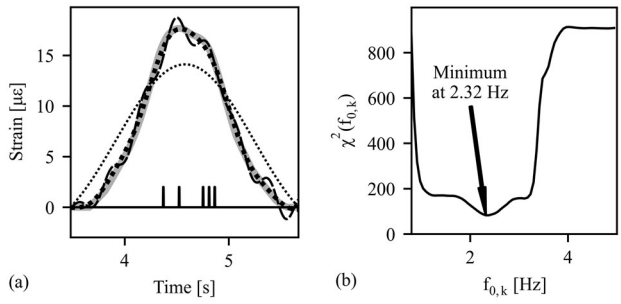

Figure 5. Example of filtering with different cut-off frequencies (a) and the minimised function (b).

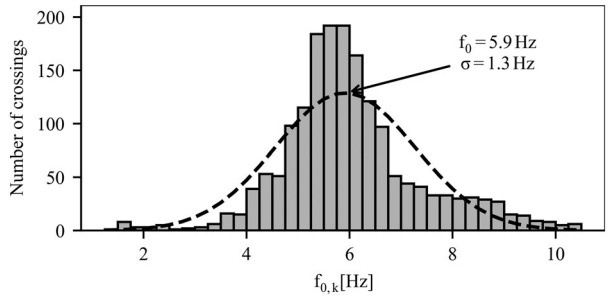

Figure 6. The histogram of cut-off frequencies and its associated Gaussian distribution for site SI05.

information content. For this reason, each lane is treated separately from the others, so that only one or a few of the most responsive sensors, with the highest signals, are used per lane (Corbally et al., 2014). If the frequencies across lanes match, the results are combined, if they do not, as was the case for the two of the test sites, they are treated separately.

Figure 5(a) depicts an estimated static response (grey), obtained by summing the individual calculated axle responses from a passage of a 5-axle semi-trailer. As an example of intermediate steps in the minimisation of equation (4), the measured signal is shown filtered with low-pass filters with different cut-off frequencies. $f_{0,k} = 0.54$ Hz is too low, and too much of the signal is filtered out, resulting in $\chi^2 = 6730$ (dotted trace). $f_{0,k} = 4.94$ Hz is too high and leaves too much of the dynamic component, with $\chi^2 = 908.5$ (dashed trace). The optimal filtering with $f_{0,k} = 2.32$ Hz produces χ^2 with the minimum value of 82.44 (thick dotted trace). The selection of optimum frequency is shown in Figure 5(b), where the dependence of χ^2 is plotted against the cut-off frequency.

This process of selecting the cut-off frequency works well for most truck crossing events but sometimes gives spurious results, in the form of excessively high or low cut-off frequencies. Consequently, the mean cut-off frequency, based on the bridge responses to all K events is calculated as:

$$f_0 = \frac{1}{K}\sum_{k=1}^{K} f_{0,k}. \tag{6}$$

Figure 6 depicts the histogram of cut-off frequencies $f_{0,k}$ for the test site SI05 described later in the article. A Gaussian distribution with the same mean and standard deviation as the measured distribution is shown superimposed on the histogram.

In the second pass, the complete dataset is filtered with the mean cut-off frequency f_0 and the DAF of the kth crossing calculated as:

$$DAF_k = \frac{\max_j g_k(t_j)}{\max_j g_k'(t_j|f_0)} = \frac{g_{k,tot}}{g_{k,qstat}}. \tag{7}$$

The DAF values determined in this manner are insensitive to the miscalculation of axle loads in individual events. Furthermore, the calculation procedure can be automated, and the B-WIM system operator does not need any knowledge of bridge dynamics.

At present, the algorithm assumes that the bridge length exceeds the longest wheelbase, and the DAF value is assigned to the vehicle as a whole. For shorter bridges, the DAF would have to be calculated from parts of the signals. Using the highest partial DAF would give a conservative estimate of the vehicle DAF.

4.4. Convergence of the first pass

To examine the convergence of calculated cut-off frequencies towards the final mean value, the partial mean $f_{0,p}$ of the initial p cut-off frequencies $f_{0,k}$ was defined as:

$$f_{0,p} = \frac{1}{p}\sum_{k=1}^{p} f_{0,k}. \tag{8}$$

and these partial means were compared with the overall mean values by defining:

$$\Delta_p = 100\ \frac{f_{0,p} - f_0}{f_0}, \tag{9}$$

which expresses the difference of partial and final means in percent. This procedure was repeated for all seventeen datasets described in the following section. The summary of the convergence analysis is presented in Figure 7.

Since the number of datasets was substantial and the graph showing individual traces would have been unreadable, the results were combined. The solid trace represents $\overline{\Delta_p}$, the mean Δ_p across all sites at $p =$ 2, 4, 8, 16, 32 … The thin grey traces are these mean values plus or minus the standard deviation across all sites at each p, and the dotted and dashed traces are the maximum and minimum values of Δ_p, respectively, across all sites.

The quick convergence is apparent. After averaging only eight values, all partial means differ by less than 5% from the final values. After 128 values, the difference drops below 2%. In practice, this means that the DAF evaluation parameters can be obtained quickly and reliably. On bridges with reasonably dense freight traffic, real-time DAF measurements can start within a few hours after the installation of a B-WIM system.

4.5. B-WIM accuracy

Accuracy evaluation procedures for WIM systems are defined in standards (ASTM-E1318-09, 2017; NMi, 2016)

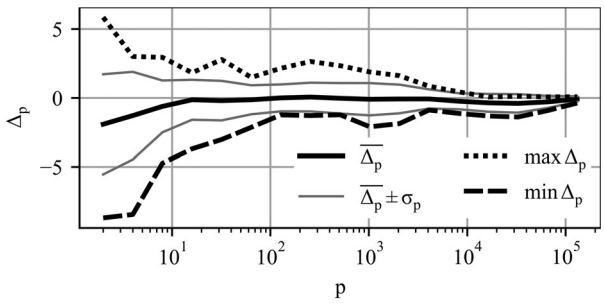

Figure 7. The convergence of $f_{0,p}$ towards the overall means.

and recommendations, such as those of the COST 323 project (Jacob et.al., 2002). In all cases, the WIM calculated axle loads and gross weight of selected vehicles are compared with their corresponding static values, usually collected with portable static scales. Systems are classified into accuracy classes based on a statistical evaluation of errors, of a few selected calibration vehicles or randomly selected vehicles from the traffic flow. Accuracy classes are defined as errors of measurement, typically at 95% confidence interval. The criteria are applied to gross weights, single axle loads and axle group loads and the system accuracy is defined as the lowest of the individual accuracies. For example, the overall classification of a system whose GVW and axle group load accuracies are A(5), but whose single axle load accuracy is B(10), will be B(10).

It should be stressed that B-WIM accuracy has no bearing on the proposed DAF calculation method since, unlike the early method (Figure 2), it does not rely on the axle loads. Decoupling of weighing and DAF calculation was the motivation for its development. The only instance where the accuracy of B-WIM results plays a role are the DAF vs GVW graphs, presented later in the text.

5. DAF measurements on selected bridges

B-WIM datasets from 15 different sites, ten from Slovenia and five from the USA, were used to validate the proposed DAF measuring methodology and to evaluate realistic DAF for bridge assessments. Sites SI01 through SI05, located on the primary and secondary state roads in Slovenia, provided 9 to 15 days of data collected during the routine B-WIM measurements. They were selected from well over 100 available datasets, based on the apparent existence of the dynamic component in bridge responses. Site SI06 was a bridge tested within a research project and for which the first few natural frequencies were measured (Kreslin, 2016). Site SI07 was a permanent test site on a motorway bridge, where a B-WIM system had been operational for over five years. Two years of data were considered in the analysis.

The bridges used to collect data on sites SI01 through SI07 were all integral reinforced concrete structures, with spans ranging from 5.5 to 12 m, while the remaining three Slovenian bridges were of the beam-and-slab type. Sites SI08 and SI09 were two parallel highway viaducts instrumented with a permanent monitoring system, including a B-WIM system. Each of the two viaducts, composed of 15 and 16 spans respectively, had simply-supported spans with four prestressed concrete beams and a continuous cast-in-place reinforced concrete deck that stretched over four spans. Finally, site SI10 was a 24.8 m long motorway single-span beam-and-slab bridge. The independent superstructures, one for each direction of traffic, of which one was instrumented, were made of five 1.4 m-deep prefabricated prestressed beams, with a 0.24 m thick reinforced concrete deck on the top. Reinforced elastic neoprene bearings supported each longitudinal beam at both ends of the bridge. Crossbeams connected the main beams over both abutments.

Table 1. Summary of the sites and results of the analysis.

					DAF		
Site	Type	Length [m]	Vehicles	f_0[Hz]	Mean	σ	Max
SI01	Slab	7.4	202	5.4	1.23	0.14	1.96
SI02	Slab	10.5	4,590	5.1	1.10	0.10	2.31
SI03	Slab	12.0	1,850	5.8	1.11	0.08	1.80
SI04a	Slab	5.5	516	9.1	1.03	0.03	1.23
SI04b	Slab	5.5	318	8.1	1.04	0.03	1.14
SI05	Slab	6.8	617	7.1	1.08	0.05	1.40
SI06a	Slab	9.7	865	5.0	1.10	0.06	1.35
SI06b	Slab	9.7	474	5.4	1.19	0.12	1.48
SI07	Slab	6.6	746,594	14.0	1.09	0.04	1.39
SI08	B&S	34.4	432,307	2.4	1.06	0.05	2.39
SI09	B&S	35.0	402,595	2.6	1.02	0.03	1.56
SI10	B&S	25.8	289,533	3.0	1.05	0.03	1.55
US01	B&S	12.2	1,979	3.5	1.05	0.04	1.34
US02	B&S	10.4	15,295	8.1	1.08	0.08	1.86
US03	B&S	11.0	7,398	8.5	1.05	0.06	1.75
US04	B&S	10.4	1,608	8.6	1.08	0.08	1.81
US05	B&S	25.0	25,219	1.6	1.17	0.13	2.37

Additionally, datasets from five highway bridges in the USA were considered, with between 16 and 23 days of data. The first four, US01 through US04, were older, multi-span structures, with 10.4 to 12.2-m long simply-supported spans, composed of four or five reinforced concrete beams or steel girders, and with reinforced concrete decks. The US05 was a 3-span highway composite underpass made of six 1.8 m high I girders and a reinforced concrete deck. Its uniqueness was the very uneven road surface in front of the bridge, which resulted in pronounced bridge vibration due to the traffic.

5.1. Selection of data

Not all vehicles were used in the analysis. For bridge loading, DAF is only relevant in conjunction with heavier vehicles. Therefore, the lower gross vehicle weight (GVW) limit at 5 tonnes was adopted. The DAF values themselves are insensitive to axle load error. However, the analysis of DAF vs GVW would have been made needlessly difficult if all the vehicles were retained.

Vehicles with unreliable axle loads, due to misidentified axles or ill-conditioned system of Equations (4), were also discarded, as were those that did not pass the data quality check (Žnidarič et al., 2018) because they had unrealistic axle loads or axle spacings, travelled at speed above 120 km/h, or if anomalies in the measured signals were detected. Finally, since this was the first application of the proposed procedure on a large selection of bridges, the measured and the calculated static strain signals of events with the highest

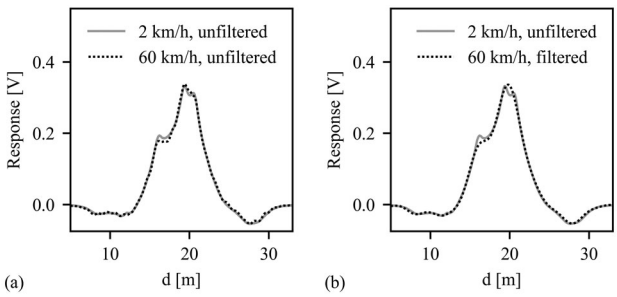

Figure 8. Comparison between static, dynamic and quasistatic responses of bridge SI06b for: (a) unfiltered and (b) filtered 60 km/h speed.

20 *DAF* s and the highest 20 GVWs were visually examined, as were the 20 heaviest discarded vehicles with unreliable axle loads. This confirmed that the extreme values were not the results of any abnormal measurements or calculations and that the discarding procedure did not eliminate correctly weighed heavy vehicles.

5.2. Results of measurements

Table 1 summarises the basic information about the test sites, the employed B-WIM datasets, and the results of DAF analyses. The 'Length' column indicates the length of the selected influence line. All of the influence lines, except in the case of the 3-span US05 bridge, covered a single span. The f_0 column contains the mean cut-off frequencies after the first data pass. The DAF columns give the calculated mean, standard deviation and maximum values of DAF after the second data pass. On sites SI04 and SI06, the two opposite lanes were treated separately and marked as 'a' and 'b' in the table, since the f_0 differed appreciably between the lanes. The probable reason for the differences was bridge asymmetry, but this was not further investigated. On other bridges, the f_0 was the same for both lanes, within the margin of error. Mean DAF values range between 1.03 and 1.23, whereas the maximum DAFs do not fall below 1.14 and can be as high as 2.39.

The basic premise of the proposed low-pass filter method is that the first natural frequency of the bridge is above the highest frequency needed to describe the static component of the bridge response. In other words, the calculated cut-off frequency needs to be lower than the first natural frequency of the bridge. Otherwise, some of the dynamic response of the bridge could be filtered out. For example, the two calculated cut-off frequencies for lanes 'a' and 'b' for site SI06 were 5.0 Hz and 5.4 Hz, and the first natural frequency on this bridge was measured at 15.5 Hz (Kreslin, 2016). Thus, for the case with known natural frequencies, the premise was verified.

The DAFs for calibration vehicles with known GVWs were examined and were found to be within one standard deviation of the mean DAF. The only exception was the site SI08, where the bridge exhibits resonance behaviour, described in the following section. The site was calibrated with three vehicles, with axle groups 1-1-3, 1-2-2 and 1-2. The mean DAFs for these vehicles were 1.05, 1.17 and 1.42, respectively. This is in agreement with the observation that this bridge is more susceptible to excitation by vehicles with particular axle groups

5.3. Validation of calculations

Data from site SI06b, used in a research project (Kreslin, 2016), was used to validate the determination of the quasi-static response. Measurements included six passes of a calibration truck at a crawling speed 2 km/h and six passes of the same vehicle at normal speed for that section of the road, 60 km/h. The truck had a single steering axle and a double driving axle, with axle distances 3.3 m and 1.35 m and axle loads 6.7 t and twice 8.6 t, making the GVW equal to 23.9 t. To remove the variance between individual runs, the six passes at each speed were averaged. Due to the slight speed variation, the signals were first transformed from time to space domain by multiplying the abscissa values with speed. The signals were aligned using cross-correlation (Press et al., 2007) and then averaged. Figure 8 shows the averaged responses at crawling and highway speed.

The solid grey trace in both figures shows the average unfiltered response of the bridge to the truck passing at a crawling speed. The dotted trace in Figure 8a displays the average dynamic bridge response due to the trucks passing at 60 km/h, while the dotted trace in Figure 8b, displays the average quasistatic bridge response, obtained by low-pass filtering the measured responses with the 5.4 Hz cut-off frequency, calculated by the algorithm. The similarity of all the traces is immediately apparent. The maxima of the static and quasistatic average responses are 332.7 mV and 336.1 mV, respectively, a difference of 1%. Therefore, in this case, using the quasistatic response leads to a 1% lower DAF compared to the static reference.

Note that the peaks of the second and the third axle, visible in the static and dynamic responses, merge into a single peak in the quasistatic response. This results from the overlapping of bridge and vehicle frequencies. The axle distance d_2 is 1.35 m. An infinite sequence of axles at such distance crossing a bridge at a speed of $v = 60\text{km/h} = 16.7\text{m/s}$ would produce a periodical response at intervals of $T = d_2/v = 0.081\text{s}$, or, equivalently, with a frequency of 12.3 Hz. At 90 km/h highway speed, the frequency of the double and triple axles increases to approximately 19 Hz. As the 5.4 Hz cut-off frequency is well below these values, any frequency-based filtering will inevitably smooth the peaks generated by the closely spaced axles.

This limitation, however, does not compromise the overall validity of the approach. To preserve the all-important components in the response of a l metre long bridge, crossed by a vehicle at a speed v, the spectrum must contain frequencies from at least v/l. Therefore, the static response of the 9.7 m long bridge SI06b, with typical speed of crossing vehicles at 60 km/h, can be described in the frequency domain with frequencies from at least 1.72 Hz. The 5.4 Hz cut-off frequency is well above this value. Calculating v/l for the 15 test sites, considering the average highway speeds, gives the frequencies that are 1.6 to 3.7 times below the respective cut-off frequencies. The proposed procedure

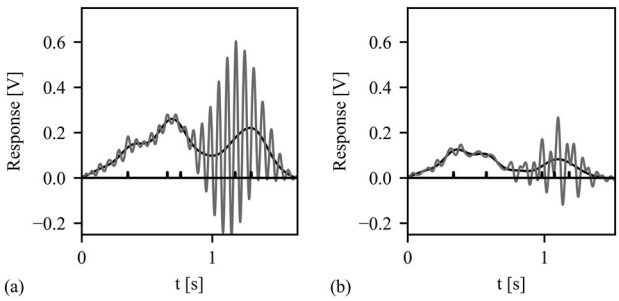

Figure 9. Two examples of high DAF values from site SI02.

thus filters out the dynamic part of the response and some of its characteristics related to the closely spaced axles, but at the same time preserves the information needed for reliable calculation of maximum quasistatic response ε_{qstat}.

5.4. Examples of DAF calculations

Figure 9 presents two typical vehicle responses from site SI02 with high DAF values. The grey and black traces are the measured and filtered signal, respectively. Figure 9(a) illustrates the vehicle with the highest DAF on this site. It had been identified as a vehicle with axle groups 1-2-1-1 (a single steering axle, followed by a twin driving axle and a trailer with two single axles), with GVW of 39.7 t and DAF equal to 2.31. A resonance effect can clearly be seen in the trailer region. The oscillation around the static values is sinusoidal, indicating a simple coupled motion.

Some strains in the measured signals can be negative. As the sensors are mounted after the bridge has been constructed, the dead load effects cannot be measured. Only the strain variation due to temperature and other environmental effects can be subtracted, to obtain the bridge response due to a vehicle crossing. Thus, the negative strains mean that the bridge deflections during the vehicle crossing are reduced compared to those of the dead load alone.

Figure 9(b) displays the passage of a 16.9 t 5-axle semi-trailer (axle groups 1-1-3) and DAF equal to 2.26. The non-sinusoidal oscillation around the static values suggests a more complex vehicle-bridge interaction. In both cases, the bridge oscillations die off as soon as the vehicles leave the bridge, which implies that the damping of this bridge is relatively high. Figure 10 shows the event with the highest GVW from this site, a 73.5 t vehicle with axle groups 1-2-2-2. In comparison to Figure 9, the dynamic component is low. This corresponds to the observation that the heaviest vehicles, in general, do not generate the highest DAFs.

Finally, Figure 11 illustrates the bridge response resulting in the highest DAF of 2.39, measured on any of the test sites. It was caused by a relatively light 20.4 t truck with axle groups 1-2-2, passing over the motorway test site SI08. The resonance effect is clearly visible. The bridge oscillations were still present in the signal eight seconds after the vehicle had left the bridge (persisting through a passage of a 1.5 t car at around seven seconds), which indicates significantly lower damping than in the case of the bridge SI02 (shown on Figure 9). The low damping is typical for such long, relatively slender, simply-supported beam-and-slab bridges. On this site, the resonance effect has been observed in all events with DAF exceeding 2. Most of them were caused by trucks with 1-2 axle configuration and GVW around 20 t or by empty tractor-trailer vehicles.

5.5. Evolution of DAF with increasing loading

One of the key findings of previous analytical and experimental work was that DAF decreases with increasing loading (Caprani, 2013; González & Žnidarič, 2009; Kirkegaard et al., 1997; Kalin et al., 2015). To examine the evolution of DAF with increasing loading, DAF_p was defined as the mean of DAF values from a subset of vehicles, whose GVW is above a cut-off point at the p^{th} percentile of the GVW cumulative distribution. For example, DAF_{10} is the mean DAF of the heaviest 90% of the vehicles, i.e., of the subset of the entire population obtained by discarding the lightest 10% of the vehicles. DAF_0 is thus the mean DAF of all the population.

For this analysis the cut-off points were chosen at the 0^{th}, 10^{th}, 20^{th} … 90^{th}, and the 95^{th} percentile. The value of DAF_{99}, calculated from the subset consisting of the heaviest 1% of vehicles, was calculated only for the four populations that numbered over 100,000 vehicles. The grouping by percentiles of GVW, rather than by GVWs themselves, allows the comparison of evolutions of DAF from all seventeen datasets with substantially different GVW ranges.

Figure 12 depicts the scatter graph of DAF vs GVW values for site SI10. All exceptional transports with GVWs above 80 t and most vehicles with GVWs above 60 t have DAF values lower than the mean DAF. The heaviest exceptional transport, weighing 113 t, had a DAF of only 1.013, making the dynamic increment in this extreme loading case approximately the same as a load effect of a car. The decreasing DAF_p trace demonstrates the apparent trend of decreasing DAF vs GVW.

Figure 13 presents the results for all seventeen datasets and the corresponding logarithmic regression curves. The abscissa displays the cut-off points in tonnes. If, due to a large amount of data, the individual data values are disregarded at this stage, the apparent observations are a) the consistent decreasing trends of DAF with GVW in all seventeen cases and b) the vast dispersion of the results. For example, at the 35-ton gross weight, matching roughly the fully-loaded vehicles, either 5-axle semi-trailers in Europe or 18-wheelers in the US, the DAF_p values vary from 1.01 on the motorway bridge SI09, to over 1.13 on the highway bridge US05.

Figure 14 illustrates the same results in a more transparent way. To combine the datasets with different GVW distributions, the abscissa was changed from the GVW cut-offs to their respective percentiles. The three curves show the DAF_p values for the three groups of bridges: from the Slovenian (SI) state roads and motorways, and US highways. Added are the linear regression curves, which in this case optimally describe the trends.

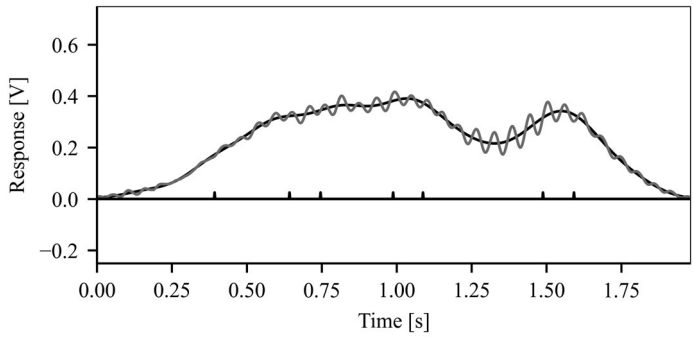

Figure 10. An example of DAF calculation from site SI02 for a very heavy special transport.

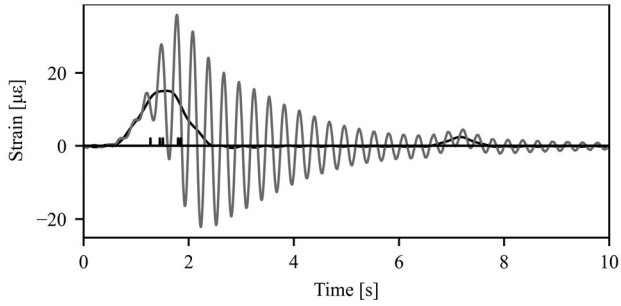

Figure 11. Event with the highest measured DAF among all vehicles from all sites.

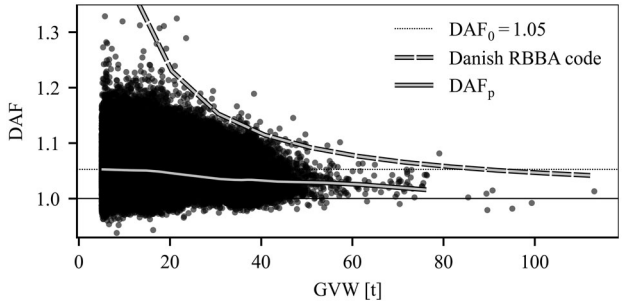

Figure 12. Scatter graph of DAF vs GVW for the highway test site SI10.

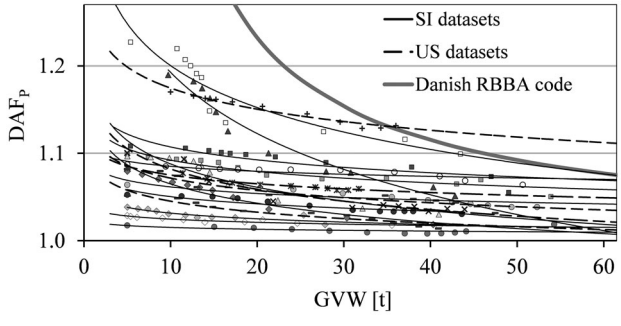

Figure 13. DAF_p versus corresponding GVW cut-offs.

Table 2 presents the results of the linear regression. The fitted slopes vary between 0.17×10^{-3}/percentile for the Slovenian motorways to 0.67×10^{-3}/percentile for the Slovenian state roads, with the US highways between these two values. The DAF_0 values for these three groups of bridges vary from 1.06 to 1.11, and the slopes yield almost identical extrapolated DAF_{100} values at the maximum (100^{th} percentile) loading, from 1.04 to 1.05.

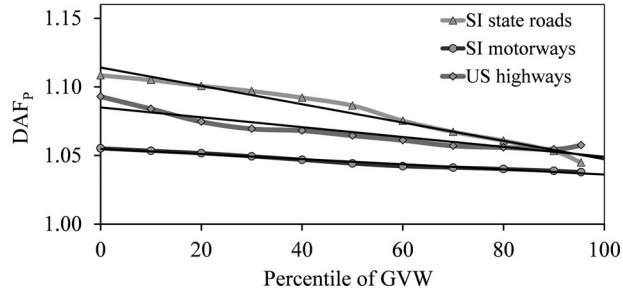

Figure 14. DAF_p as a function of GVW percentile for three groups of bridges.

Table 2. : Results of linear regression on the DAF_p curves.

	SI state roads	US highways	SI motorways
DAF_0	1.11	1.09	1.06
Slope	-0.67×10^{-3}	-0.36×10^{-3}	-0.17×10^{-3}
DAF_{100}	1.05	1.05	1.04

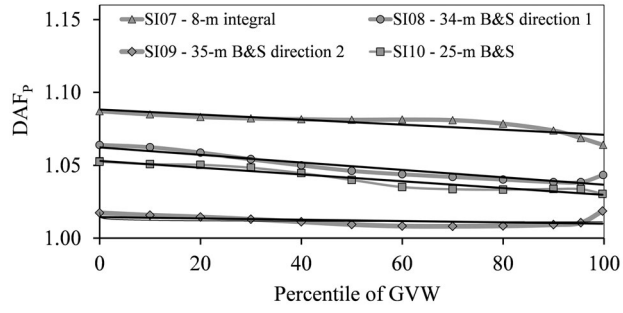

Figure 15. DAF_p for the four Slovenian motorway bridges.

The individual data set results are less consistent. Figure 15 details the four Slovenian motorway bridges. The results differ significantly, most notably between the two nearly identical beam-and-slab bridges SI08 and SI09, renovated in 2018 and 2019, respectively.

An inspection of the events with highest DAF values on the bridge SI08 revealed that all resulted from the resonance effects, such as shown in Figure 11. A closer investigation of the two bridges suggested the possible cause of the different behaviours. The estimated first natural frequencies of both bridges were similar, 3.5 Hz and 3.3 Hz, respectively, near the typical whole vehicle body bounce frequency of 3 Hz (Cebon, 1999). The main difference was the expansion joint just before the instrumented span of SI08, the most likely trigger for the frequent resonance effects, by exciting

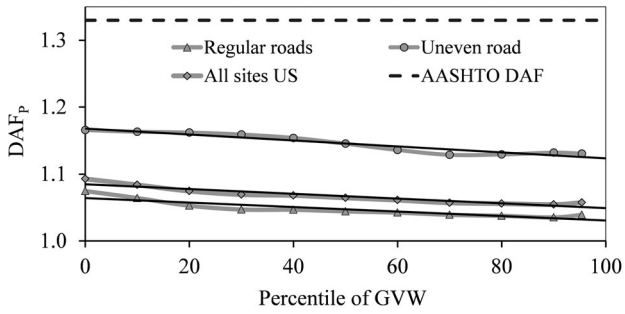

Figure 16. DAF_p for the five US highway bridges.

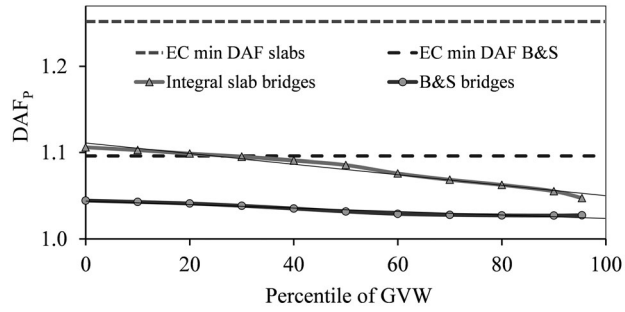

Figure 17. DAF_p for Slovenian bridges divided by structural type.

Table 3. Statistics of events with the 10 highest DAFs.

Site	Max. DAF	at GVW [t]	Max. GVW_{dyn}	Mean DAF	Mean GVW [t]
SI01	1.96	13.7	26.9	1.61	14.3
SI02	2.31	39.8	91.9	2.14	22.2
SI03	1.80	38.8	69.8	1.58	29.8
SI04a	1.23	24.6	30.3	1.13	10.3
SI04b	1.14	8.2	9.3	1.12	7.0
SI05	1.40	5.1	7.1	1.26	8.8
SI06a	1.35	8.6	11.6	1.28	12.5
SI06b	1.48	15.7	23.2	1.43	18.3
SI07	1.39	17.9	24.9	1.31	20.4
SI08	2.39	22.5	53.8	2.17	19.5
SI09	1.56	5.3	8.3	1.45	7.8
SI10	1.55	10.0	15.5	1.33	13.2
US01	1.34	8.3	11.1	1.27	13.6
US02	1.86	13.4	24.9	1.79	13.0
US03	1.75	18.4	32.2	1.56	15.6
US04	1.81	20.9	37.8	1.38	15.9
US05	2.36	11.7	27.6	2.15	16.5

vehicles' body bounce mode of vibrations just prior to arrival on the bridge. The structurally identical, only 0.6 m longer site SI09, with no expansion joint before the instrumented span, did not exhibit any similar resonance behaviour.

Figure 16 elaborates the trends observed on the US highway bridges. While the DAF values of the first four were similar, significantly higher dynamic loading was measured on the three-span highway underpass US05. This bridge had an extremely uneven pavement at its entrance, with deep potholes and loose aggregate from the wearing course. The graph also shows the 1.33 allowance, according to the 2017 AASHTO specifications. This value is far above the mean measured values.

Finally, Figure 17 displays the trends for the two bridge structural types tested in Slovenia, the integral slab bridges and the beam-and-slab bridges. The results are compared with the 2-lane traffic allowances, integrated into the Eurocode load model 1 (Figure 1). Again, all measured DAF_p values are well below those from the code. As the Eurocode DAF values depend on the bridge span, Figure 17 displays the minimum allowances, for the span length between 5.5 and 12.0 metres for the slab bridges, and between 24.8 and 35.4 m for the beam-and-slab bridges.

5.6. Events with the highest DAF values

Since the extreme DAF values do not result from the heaviest vehicles, it is worthwhile to analyse the events that caused the highest values of DAFs. Table 3 summarises the maximum and mean values of DAF and GVW for ten such events from all seventeen datasets. The maximum DAF values are matched with the corresponding vehicle gross weight and the mean DAF values are compared with the corresponding mean GVW value. The first observation is that precisely one vehicle out of 170, a 41.4 t truck on site SI03, with axle groups 1-3-3, exceeded the legal load of 40 tonnes.

The bridge most vulnerable to the total dynamic loading, i.e. the product of GVW and DAF, turned to be the 10.5-m long bridge SI02, where the maximum dynamic loading GVW_{dyn} corresponded to a 92-tonne vehicle. GVW_{dyn} is only a rough estimate of heavy traffic loading, which includes dynamics. For more precise analysis the axle loads would have to be converted into load effects. The values on all other bridges were considerably lower. Only on sites SI03 and SI08 did the maximum GVW_{dyn} and the product of the mean values of DAF and GVW exceeded the static weight of a fully-loaded freight vehicle. On all other sites, the maximum dynamic excitations were triggered by considerably lighter vehicles. In fourteen cases the mean GVW of vehicles in the ten most dynamic events was below 20 tonnes, in three cases even below 10 tonnes.

6. Conclusions

This article presented the procedure for calculation of bridge dynamic amplification factor from B-WIM measurements. An automated method that calculates DAF values from all bridge heavy vehicle crossing events was described. The most significant advancement compared to previous attempts is that it applies a two-pass calculation procedure. This approach removes the need for an expert who selected the parameters based on personal experience. The DAF values for this article were calculated from the bridge flexural strains. However, there is nothing in the two-pass method that would inherently preclude the use for calculation of DAFs for other observed quantities of interest, such as bridge deflection or shear deformations.

To verify the calculation procedure and to test the hypothesis that the DAF decreases with increasing loading, the most extensive test so far of measured DAF was performed. The results obtained from seventeen selected datasets from Slovenia and USA are in accordance with the observations of the existing theoretical studies and the

results of previous research: almost without exceptions, the highest DAF values were triggered by vehicles of relatively low gross weight and were associated with some sort of resonance effect. The method proved to be robust and reliable. All empirical validations of the extreme values indicated that the measurements and the subsequent processing were valid and that the DAF values were correct. The method was also validated by comparing the static response of the bridge at crawling speed and the corresponding filtered dynamic response at normal driving speed. The convergence test suggested that less than 100 freight vehicle records are sufficient to set the parameters for real-time DAF measurements.

Finally, the findings also confirm that bridge and vehicle characteristics, and the resulting vehicle-bridge interaction play a crucial role in dynamic bridge loading. As suggested by high differences between DAFs for two structurally almost identical bridges, SI08 and SI09, the details of the approach to the bridge are a possibly large influence on the subsequent dynamic behaviour of the vehicle-bridge system. For the 17 considered datasets, the ratio between the highest and lowest measured DAF factors for the heaviest vehicles was almost 12. For this reason, as already suggested in the literature (Žnidarič et al., 2006), it is difficult to recommend a general reduction of DAF for bridge assessment below 1.15. However, if B-WIM results are available, further DAF analysis may reveal substantial additional reserves for the analysed bridge, which can play a decisive role in the duration and cost of the selected measures.

Acknowledgements

The authors would like to express their gratitude for the support received from the Slovenian Research Agency programme P2-0273 Building Structures and Materials, as well as to the Slovenian Infrastructure Agency, the Motorway Company of Slovenia DARS d.d. and Cestel d.o.o., for providing access to the weigh-in-motion data.

Disclosure statement

No potential conflict of interest was provided by the author(s).

Funding

This study was funded by Javna Agencija za Raziskovalno Dejavnost RS.

ORCID

Jan Kalin http://orcid.org/0000-0001-5704-9276
Aleš Žnidarič http://orcid.org/0000-0002-1526-2519
Andrej Anžlin http://orcid.org/0000-0002-3626-7204

References

AASHTO (1928). *Standard specifications for highway bridges and incidental structures*. USA: American Association of State Highway and Transportation Officials.

AASHTO (1989). *Guide specifications for strength evaluation of existing steel and concrete bridges*. USA: American Association of State Highway and Transportation Officials.

AASHTO (1996). *Bridge Design Specifications*. USA: American Association of State Highway and Transportation Officials.

AASHTO (2017). *Bridge Design Specifications* 8th Ed. USA: American Association of State Highway and Transportation Officials.

Alois, B., Croce, P., Sanpaolesi, L., & Gerhard, S. (1996). ENV1991-Part 3: Traffic loads on bridges. Calibration of road load models for road bridges. *Proceedings of IABSE Colloquium*, Vol. 74, 439– 453.

Bakht, B., & Pinjarkar, S. G. (1989). Dynamic testing of highway bridges–a review. *Transportation Research Record*, *1223*, 93–100.

Cantero, D., González, A., & O'Brien, E. J. (2009). Maximum dynamic stress on bridges traversed by moving loads. *Bridge Engineering*, *162*, 75–85.

Cantieni, R. (1984). *Dynamic load tests on highway bridges in Switzerland – 60 Years experience of EMPA*. Swiss Federal Laboratories for Materials Testing and Research, Dübendorf, Switzerland.

Caprani, C. (2005). *Probabilistic Analysis of Highway Bridge Traffic Loading* (Ph.D. Thesis). UCD

Caprani, C. (2013). *Lifetime Highway Bridge Traffic Load Effect from a Combination of Traffic States Allowing for Dynamic Amplification*. *Journal of Bridge Engineering*, *18*(9), 901–909. https://doi.org/10.1061/. (ASCE)BE.1943-5592.0000427 doi:10.1061/(ASCE)BE.1943-5592.0000427

Casas, J. R., Olaszek, P., Šajna, A., Žnidarič, A., & Lavrič, I. (2009). Recommendations on the Use of Soft, Diagnostic Or Proof Load Testing: ARCHES deliverable D16 3-7, *European Commission*,

Cebon, D. (1999). *Handbook of Vehicle-Road Interaction*. Abingdon: Taylor & Francis.

CEN (2003). *Eurocode 1: Actions on structures – Part 2: Traffic loads on bridges* (SIST EN 1991-2:2004), SIST - Slovenski inštitut za standardizacijo, Ljubljana, Slovenija.

Corbally, R., Žnidarič, A., Cantero, D., Haijalizadeh, D., Leahy, C., Kalin, J. & Kreslin, (2014). *Algorithms for Improved Accuracy of Static Bridge-WIM Systems: BridgeMon D3. 1 report*. European Commission

DRD (2004). Reliability-Based Classification of the Load Carrying. Danish Roads Directorate *Capacity of Existing Bridges*. *Guideline Document* (Report 291), Copenhagen.

Ghosn, M., & Xu, Q. (1989). Estimating Bridge Dynamics Using the Weigh-in-Motion Algorithm. *Transportation Research Record*, *1200*, 7–14.

González, A., & Mohammed, O. (2018). Dynamic Amplification Factor of Continuous versus Simply Supported Bridges Due to the Action of a Moving Vehicle. *Infrastructures*, *3*(2), 12. doi:10.3390/infrastructures3020012

González, A., & Žnidarič, A. (2009). *Recommendations on dynamic amplification allowance: ARCHES deliverable D10*, 75. *European Commission*,

Humar, J. L., & Kashif, A. H. (1995). Dynamic response analysis of slab-type bridges. *Journal of Structural Engineering*, *121*(1), 48–62. https://doi.org/10.1061/. (ASCE)0733-9445(1995)121:1(48) doi:10.1061/(ASCE)0733-9445(1995)121:1(48)

Jacob, B., O'Brien, E. & Jehaes, (2002). Weigh-in-Motion of Road Vehicles: Final Report of the COST 323 action, Brussels.

Kalin, J., Žnidarič, A., & Kreslin, M. (2015). *Using weigh-in-motion data to determine bridge dynamic amplification factor*. EVACES'15, 6th International Conference on Experimental Vibration Analysis for Civil Engineering Structures. doi:10.1051/matecconf/20152402003

Kirkegaard, P. H., Neilsen, S. R. K., & Enevoldsen, I. (1997). *Heavy vehicles on minor highway bridges - calculation of dynamic impact factors from selected crossing scenarios*. Aalborg: Department of Building Technology and Structural Engineering, Aalborg University.

Kingdom of Yugoslavia. (1936). *Regulations for road bridges: Appendix: Dynamic Amplification Factor, 2. October 1936*. In Serbian. Retrieved from Belgrade.

Kreslin, M. (2016). *Influence of road surface unevenness on accuracy of bridge weigh-in-motion results*. In: Research Project funded by Slovenian Research Agency.

McLean, D. I., & Marsh, M. L. (1998). *Dynamic impact factors for bridges*. Transportation Research Board.

Ministry of Transportation and Communication. (1983). Ontario highway bridge design code, Ontario

Moses, F. (1979). Weigh-in-motion system using instrumented bridges. *Journal of Transportation Engineering*, *105*(3), 233–249.

Nassif, H. H., & Nowak, A. S. (1995). Dynamic Load Spectra for Girder Bridges. *Transportation Research Record*, *1476*, 69–83.

Nassif, H. H., & Nowak, A. S. (1996). Dynamic load for girder bridges under normal traffic. *Archives of Civil Engineering*, *42*(4), 381–400.

O'Brien, E. J., & Žnidarič, A. (2001). *Report of WAVE project Work Package 1.2 - Bridge WIM*, Dublin, Ljubljana: UCD & ZAG

Press, W. H., Teukolsky, S. A., Vetterling, W. T., & Flannery, B. P. (2007). *Numerical recipes 3rd edition: The art of scientific computing*: Cambridge university press, Cambridge, UK.

Wright, D. T., & Green, R. (1964). *Highway Bridge Vibrations: Part II, Ontario Test Programme*. Department of Civil Engineering, Queen's University, Kingston, Ontario, Canada.

Žnidarič, A., Kalin, J., & Kreslin, M. (2018). Improved accuracy and robustness of bridge weigh-in-motion systems. *Structure and Infrastructure Engineering*, *14*(4), 412–424. doi:10.1080/15732479.2017.1406958

Žnidarič, A., & Kalin, J. (2020). Using Bridge Weigh-in-Motion Systems to Monitor Single-Span Bridge Influence Lines. *Journal of Civil Structural Health Monitoring*, *10*(5), 743–756. doi:10.1007/s13349-020-00407-2

Žnidarič, A., & Lavrič, I. (2010). *Applications of B-WIM technology to bridge assessment*. (pp. 1001–1008). Philadelphia, PA: Proceedings of IABMAS 2010 Conference.

Žnidarič, A., Lavrič, I., & Kalin, J. (2008). *Measurements of bridge dynamics with a bridge weigh-in-motion system*. 5th International Conference on Weigh-in-Motion (ICWIM5).

Žnidarič, A., Lavrič, I., & Kalin, J. (2010). *Latest practical developments in the Bridge WIM technology* (pp. 993–1000Philadelphia, PA: Proceedings of IABMAS 2010 Conference.

Žnidarič, A., O'Brien, E., Casas, J., O'Connor, A., Wierzbicki, T., Lavrič, I., & Kalin, J. (2006). *Guidance for the Optimal Assessment of Highway Structures: SAMARIS deliverable D30.* European Commission.